

# Middlesex University Research Repository

An open access repository of

Middlesex University research

<http://eprints.mdx.ac.uk>

Sophocleous, L., Frerichs, Inez, Miedema, M., Kallio, M., Papadouri, T., Karaoli, Christina, Becher, T., Tingay, David, van Kaam, Anton, Bayford, Richard ORCID logo ORCID: <https://orcid.org/0000-0001-8863-6385> and Waldmann, Andreas D. (2018) Clinical performance of a novel textile interface for neonatal chest electrical impedance tomography. *Physiological Measurement*, 39 (4) , 044004. ISSN 0967-3334 [Article] (doi:10.1088/1361-6579/aab513)

Final accepted version (with author's formatting)

This version is available at: <https://eprints.mdx.ac.uk/24283/>

## Copyright:

Middlesex University Research Repository makes the University's research available electronically.

Copyright and moral rights to this work are retained by the author and/or other copyright owners unless otherwise stated. The work is supplied on the understanding that any use for commercial gain is strictly forbidden. A copy may be downloaded for personal, non-commercial, research or study without prior permission and without charge.

Works, including theses and research projects, may not be reproduced in any format or medium, or extensive quotations taken from them, or their content changed in any way, without first obtaining permission in writing from the copyright holder(s). They may not be sold or exploited commercially in any format or medium without the prior written permission of the copyright holder(s).

Full bibliographic details must be given when referring to, or quoting from full items including the author's name, the title of the work, publication details where relevant (place, publisher, date), pagination, and for theses or dissertations the awarding institution, the degree type awarded, and the date of the award.

If you believe that any material held in the repository infringes copyright law, please contact the Repository Team at Middlesex University via the following email address:

[eprints@mdx.ac.uk](mailto:eprints@mdx.ac.uk)

The item will be removed from the repository while any claim is being investigated.

See also repository copyright: re-use policy: <http://eprints.mdx.ac.uk/policies.html#copy>

# Clinical performance of a novel textile interface for neonatal chest electrical impedance tomography

L Sophocleous<sup>1</sup>, I Frerichs<sup>2</sup>, M Miedema<sup>3</sup>, M Kallio<sup>4</sup>, T Papadouri<sup>5</sup>,  
C Karaoli<sup>5</sup>, T Becher<sup>2</sup>, DG Tingay<sup>6-8</sup>, A van Kaam<sup>3</sup>, R Bayford<sup>9</sup> and  
AD Waldmann<sup>10</sup>

<sup>1</sup> KIOS Research Centre, Department of Electrical and Computer Engineering, University of Cyprus, Nicosia, Cyprus  
<sup>2</sup> Department of Anaesthesiology and Intensive Care Medicine, University Medical Centre Schleswig-Holstein, Campus Kiel, Kiel, Germany  
<sup>3</sup> Department of Neonatology, Emma Children's Hospital, Academic Medical Centre Amsterdam, Amsterdam, The Netherlands  
<sup>4</sup> PEDEGO Research Group, University of Oulu and Department of Children and Adolescents, Oulu University Hospital, Oulu, Finland  
<sup>5</sup> Neonatal Intensive Care Unit, Arch. Makarios III Hospital, Nicosia, Cyprus  
<sup>6</sup> Neonatal Research, Murdoch Childrens Research Institute, Parkville, Victoria, Australia  
<sup>7</sup> Department of Paediatrics, University of Melbourne, Melbourne, Australia  
<sup>8</sup> Neonatology, Royal Children's Hospital, Parkville, Australia  
<sup>9</sup> Department of Natural Sciences, Middlesex University, London, UK  
<sup>10</sup> Swisstom, Landquart, Switzerland

E-mail: awa@swisstom.com

**Abstract.**

*Objective:* Critically ill neonates and infants might particularly benefit from continuous chest electrical impedance tomography (EIT) monitoring at the bedside. In this study a textile 32-electrode interface for neonatal EIT examination has been developed and tested to validate its clinical performance. The objectives were to assess ease of use in a clinical setting, stability of contact impedance at the electrode-skin interface and possible adverse effects. *Approach:* Thirty preterm infants (gestational age: 30.3±3.9 wk (mean ± SD), postnatal age: 32.3±4.4 wk, body weight at inclusion: 1727±869 g) were included in this multicentre study. The electrode-skin contact impedances were measured continuously for up to three days and analysed during the initial 20-min phase after fastening the belt and during a 10-hour measurement interval without any clinical interventions. The skin condition was assessed by attending clinicians. *Main results:* Our findings imply that the textile electrode interface is suitable for long-term neonatal chest EIT imaging. It does not cause any distress for the preterm infants or discomfort. Stable contact impedance of about 300 Ohm was observed immediately after fastening the electrode belt and during the subsequent 20-min period. A slight increase in contact impedance was observed over time not affecting the functional EIT image generation. Tidal variation of contact impedance was less than 5 Ohm. *Significance:* The availability of a textile 32-electrode belt for neonatal EIT imaging with simple, fast, accurate and reproducible placement on the chest strengthens the potential of EIT to be used for regional lung monitoring in critically ill neonates and infants.

Keywords: EIT, electrical impedance, respiratory system, contact impedance, neonatal lung imaging, EIT belt, electrodes, CRADL

## 1. Introduction

Continuous assessment of regional lung function using electrical impedance tomography (EIT) in critically ill neonates and infants has recently received much research interest (Frerichs *et al* 2017). Several characteristics advocate EIT as a monitoring tool in neonatal intensive care units (NICU). EIT allows the estimation of electrical impedance distribution in part of the chest by injecting a small alternating current at high frequencies through electrodes placed on the chest circumference. From the measured voltages on the surface, assessment of the electrical impedance of the tissues contained within the chest can be made. EIT has a very high temporal resolution since it operates at 10-50 images per second (Bayford 2006).

EIT was identified as a potentially promising thoracic imaging technology early in the development of EIT systems (Brown *et al* 1985) even though it suffered from low spatial resolution. The vulnerable population of preterm infants is particularly suited for EIT monitoring. EIT is non-invasive, does not use ionising radiation, can be performed at the bedside and provides continuous information. Therefore it offers several advantages compared to traditionally used imaging techniques such as chest radiography (Chatziioannidis *et al* 2011, Adler *et al* 2012, Frerichs *et al* 2017). Nonetheless, EIT is not yet adopted for regular use in a clinical NICU setting.

One obstacle for routine EIT applications in critically ill neonates and infants comes from the ergonomic problems associated with the placement of single electrodes around the neonatal chest with equidistant spacing which requires extensive handling (Hampshire *et al* 1995, Taktak *et al* 1995, Frerichs *et al* 2003, Dunlop *et al* 2006, Chatziioannidis *et al* 2011, Miedema *et al* 2012). Early studies on EIT imaging of the neonatal lung suggested that an electrode belt could be a significant improvement for electrode placement (Hampshire *et al* 1995). However, more than 20 years passed until the first approved EIT electrode belt became available for the use in small infants. As highlighted in the recent summary of EIT applications in neonates, infants and children (Frerichs *et al* 2017) such a single EIT patient interface could accelerate the implementation of EIT in routine neonatal care. It was also stated that this interface had to be specifically designed for this patient population making simple one-to-one miniaturization of the existing adult EIT interfaces impossible. The neonatal EIT belt should not compromise chest expansion but still guarantee good and stable electrode contact without any adverse effects. Furthermore, low electrode-skin impedance is essential since electrodes in EIT are used for both voltage measurements and current injections (Rahal *et al* 2009). High contact impedance values in the circuit for voltage measurement reduce the common-mode rejection ratio (CMMR), whereas high contact impedance values in the circuit for current injection lead to high values of common-mode voltage (McAdams *et al* 1996, Boyle and Adler 2011, Adler *et al* 2015).

In this study a textile electrode interface for neonatal EIT measurement has been developed and tested to validate its clinical performance in a multicentre clinical study. Our aim was to assess ease of use in a clinical setting, stability of contact impedance at the electrode-skin interface and possible adverse effects.

## 2. Methods

### 2.1. Study population and protocol

This study was performed within the framework of a larger multicentre observational study called Continuous Regional Analysis Device for neonate Lung (CRADL) analysing whether EIT has the potential to optimise the ventilator therapy in neonatal and paediatric patients (NCT02962505). With the approval of the responsible ethics committees and after obtaining written informed consent of both parents, 30 infants were included in total from the Emma Children's Hospital, Amsterdam, Netherlands (Ethics number: METC 2016/184), the Arch. Makarios III Hospital,

Nicosia, Cyprus (Ethics number: EEBK/EP/2016/32) and the Oulu University Hospital, Oulu, Finland (Ethics number: EETTMK 35/2017).

Infants with a body weight less than 600 g, postmenstrual age less than 25 weeks at inclusion, electrically active implants or those suffering from thorax skin lesions were excluded from the study. In the NICU, the electrode-skin contact impedances were continuously measured during a maximal time period of 72 hours or until the infants were discharged either to another department or home. Events such as body position change, patient care, extubation and belt removal, for example during imaging or kangaroo care, were entered into the study software. Attending clinicians were instructed to report observed skin irritations or suspected restriction of breathing caused by the neonatal belt during the entire recording. Their findings were assessed using a questionnaire with four questions with either the Likert rating scale or multiple-choice responses (Appendix). Extra space was added to write additional comments. At the beginning of the protocol, infants were positioned supine, the circumference below the nipple line was measured and appropriate belt selected. Commonly used neonatal ultrasound gel (Aquasonic 100, Parker Laboratory Inc, USA) was applied to the belt before fastening along the 5-6<sup>th</sup> intercostal space. Thereafter the patients were treated according to local standards of care.

2.2. EIT device

EIT measurements were performed with the CRADL study EIT device (Swisstom AG, Landquart, Switzerland). This is a 32-electrode EIT system using a skip four pattern of electrical current applications and voltage measurements. The current injection amplitude is 3 mA<sub>rms</sub> at a frequency of 200 kHz. Electrode-skin contact impedances were measured at the current injecting electrode pair. The measured electrode-skin contact impedance included the junction between electrode and skin, the skin impedance and part of the body tissue between the two electrodes. The compliance voltage of the system, defined as the maximal voltage that the current source can supply to a load, was 6 Volt.

2.3. Neonatal electrode belt

The textile electrode belt comprises a striped electrically conductive textile cover and a three-dimensional space fabric wrapped around a flexible printed circuit board carrying 32 electrode contacts (figure 1). One conductive strip of a silver-coated yarn separated by non-conductive polyester fabric (X-static, Noble Materials, USA) is in electrical contact with the skin at one end and the flexible circuit board at the other. The spacer fabric ensures thermo-physiological comfort for the neonatal skin. A soft closing strap and a Velcro fasten the belt around the neonatal chest. An orientation symbol helps the clinicians to correctly place the neonatal electrode belt.

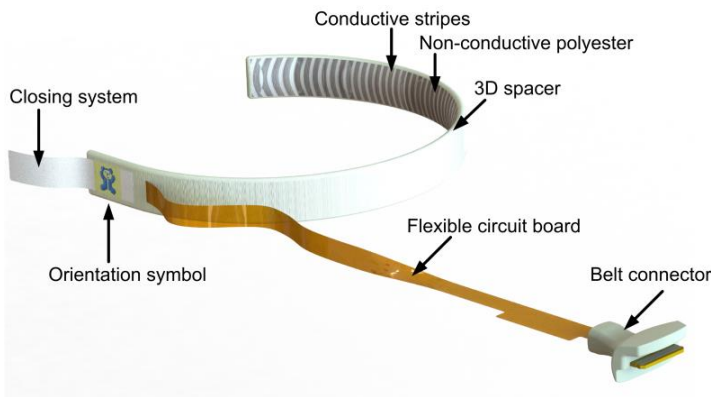


**Figure 1** Neonatal electrode belt consists of a striped electrically conductive textile, a three-dimensional space fabric, an ultra-flexible printed circuit board and a Velcro based closing system. Each of the 32 electrodes has a size of 1 cm<sup>2</sup>.

Belts in 5 different sizes – 17.5 cm, 20 cm, 23.5 cm 27.5 cm and 33 cm – were produced to cover the chest circumferences between 17 and 36 cm. Figure 2 gives an example chest X-ray with the belt positioned on the chest of one of the infants enrolled in the study.

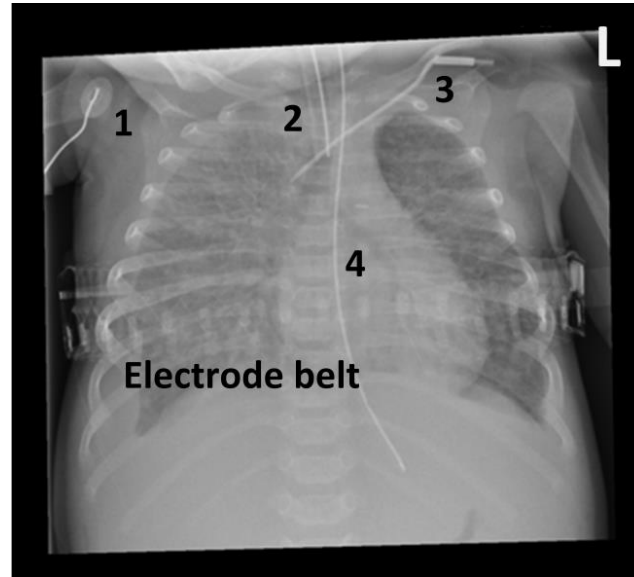


**Figure 2.** Chest X-ray image of a patient with the belt fastened around the thorax. 1) ECG electrode, 2) endotracheal tube, 3) central venous line, 4) nasogastric tube.

#### 2.4 Data analysis

Data processing and analysis was carried out off-line using Matlab (Mathworks, Nantick, MA, USA). Descriptive statistics were used to summarise the results of the questionnaires. Results are presented in table 1 together with the patients' characteristics.

In order to evaluate the stability of the electrode-skin contact impedance, we analysed a one-minute recording immediately after fastening the belt, and then five-minutely for the subsequent 20 minutes. Results are presented in boxplots as mean values of all electrodes for each patient. The 16 ventral and 16 dorsal electrodes were analysed separately to examine the possible effect of gravity.

Test for normality was performed using the Shapiro-Wilk test. Data from the ventral and dorsal hemithoraces were compared for each minute using one-way analysis of variance (ANOVA) and Student's paired t-test.  $p$  values  $< 0.05$  were considered statistically significant. Repeated measures ANOVA were done on the ventral and dorsal data separately over time. In a second step, we analysed the contact impedance changes during tidal ventilation for each electrode in each patient. The differences between the contact impedances at the start and end of inspiration were calculated for each tidal inflation. The values of 10 consecutive stable inflations were then averaged.

For the assessment of the long-term performance and possible drying out of the gel, we analysed the contact impedance during a time period of up to 10 hours. A sequence without belt removal or gel application was selected for each patient. Then we selected a data sequence until the mean contact impedance decreased for the first time. Afterwards the mean contact impedance of all 32 electrodes was calculated for each patient during 30 minutes and the results were plotted in boxplots.

Electrodes with skin contact impedance higher than 700 Ohm were excluded from the analysis, marked as "failing" and treated separately. The threshold of 700 Ohm was defined according to the manufacturer's specifications.

3. Results

The novel textile patient interface was used on 30 patients during EIT measurements between 24 and 72 hours (table 1). 20 Patients were recorded during 72 hours, while for the other 10 patients the recordings were stopped earlier and the patients were either discharged home or to another department within the hospital. None of the recordings was interrupted or stopped because of the EIT belt. Results of the questionnaires revealed that the belts did not lead to restrictions of breathing in any of the patients (table 1). Six of the 30 observed patients exhibited minor skin irritations close to where the belt was fastened. All skin irritations disappeared within less than one hour after removing the belt.

Table 1: Patient data and results from questionnaires.

Subject number	Gestational age (weeks)	Postnatal age (weeks)	Weight at inclusion (g)	Chest circumference (cm)	Belt size (cm)	Examination time (h)	Breathing restriction	Skin condition
1	30.0	30.3	1470	26	23.5	50	no	no
2	36.0	36.4	2710	30	27.5	72	no	no
3	28.7	30.3	1360	26	23.5	61	no	no
4	29.9	30.4	1330	26	23.5	35	no	no
5	34.3	34.4	1975	28	27.5	49	no	minor redness
6	31.0	32.8	1895	28	27.5	46	no	minor redness
7	29.8	30.1	2030	27	27.5	72	no	no
8	27.6	29.3	1240	23	20	72	no	no
9	28.8	31.4	1340	24	23.5	72	no	minor redness
10	27.1	30.7	1375	23	23.5	72	no	no
11	28.1	30.1	1395	25	23.5	72	no	no
12	28.1	28.1	1340	25	23.5	72	no	no
13	24.3	46.4	4035	35	33	27	no	no
14	42.1	44.4	4080	36	33	24	no	minor redness
15	27.5	32.1	1580	27	23.5	44	no	minor redness
16	29.1	29.7	1275	23.5	20	42	no	no
17	26.1	31.6	1430	24	23.5	41	no	no
18	29.7	30.7	958	23	20	72	no	no
19	30.7	31.1	1136	23	23.5	72	no	no
20	28.1	29	833	23	23.5	72	no	no
21	28	29	1028	23	23.5	72	no	no
22	29	29.8	1440	24	23.5	72	no	no
23	33.5	34	1880	27.5	27.5	72	no	no
24	30	30.4	1300	23	23.5	72	no	no
25	27	28.4	880	20	20	72	no	no
26	27.3	27.8	1090	23	23.5	72	no	no
27	36.1	36.8	3000	31	27.5	72	no	no
28	28.1	29	810	21	20	72	no	no
29	38	38.1	2800	31	33	72	no	no
30	35.4	35.3	2815	30.5	27.5	60	no	minor redness
Mean	30.3	32.3	1727.0	26.0	---	61.5	---	---
SD	3.9	4.4	869.1	3.8	---	15.6	---	---

Immediately after fastening the electrode belt the mean contact impedance values approximated 300 Ohm. There was no statistically significant increase in contact impedance during the first 20 minutes of recording as determined by repeated measures ANOVA (dorsal  $F(4,116)=0.97$ ,  $p=0.42$ , ventral  $F(4,116)=0.91$ ,  $p=0.45$ ). The number of failing electrodes, having contact impedance higher than 700 Ohm, was 0.3% right after fastening the belt and increased to 0.5% after 20 min of recording. In 25 patients no failing electrodes were detected in the first 20 minutes. The other patients showed failing electrodes at least once in this period. The dorsal electrodes showed significantly lower contact impedances compared to the ventral electrodes during the first 20 min of recording.

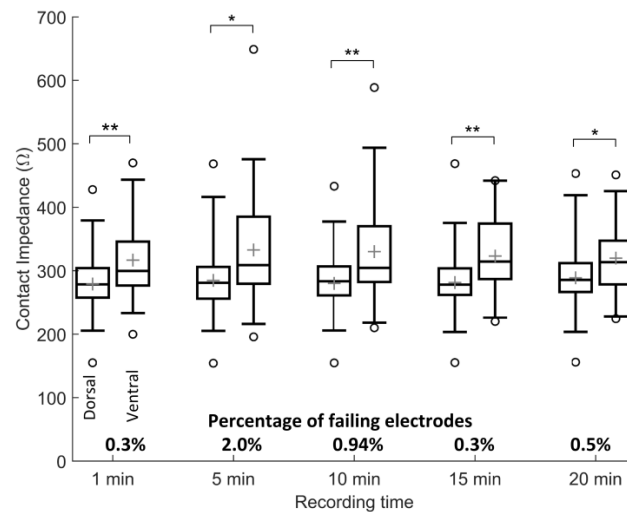


**Figure 3.** Boxplots of skin contact impedances at all-time points (n=30 infants in supine position). The contact impedances of the ventral and dorsal electrodes are depicted separately. Boxes indicate 25<sup>th</sup>-75<sup>th</sup> percentiles; the median values are depicted by the lines within the boxes, and the mean values by crosses. The whiskers mark the 5<sup>th</sup> and 95<sup>th</sup> confidence interval. \*  $p < 0.05$  and \*\*  $p < 0.01$  for differences between the dorsal and ventral electrodes. The percentage of failing electrodes at each time point is shown below the corresponding boxplot.

Figure 4 shows a representative ventilation signal measured by the EIT device in one infant. The measured voltage increases during inspiration and decreases during expiration (panel A). The simultaneously measured contact impedance changes slightly during tidal ventilation. The contact impedance changes in the ventral part (panel B) are marginally higher, compared to the dorsal ones (panel C). In most of the patients, the changes are less than 5 Ohm for all 32 electrodes (panel D). Most of the electrodes show higher contact impedances at end of inspiration compared to start of inspiration.

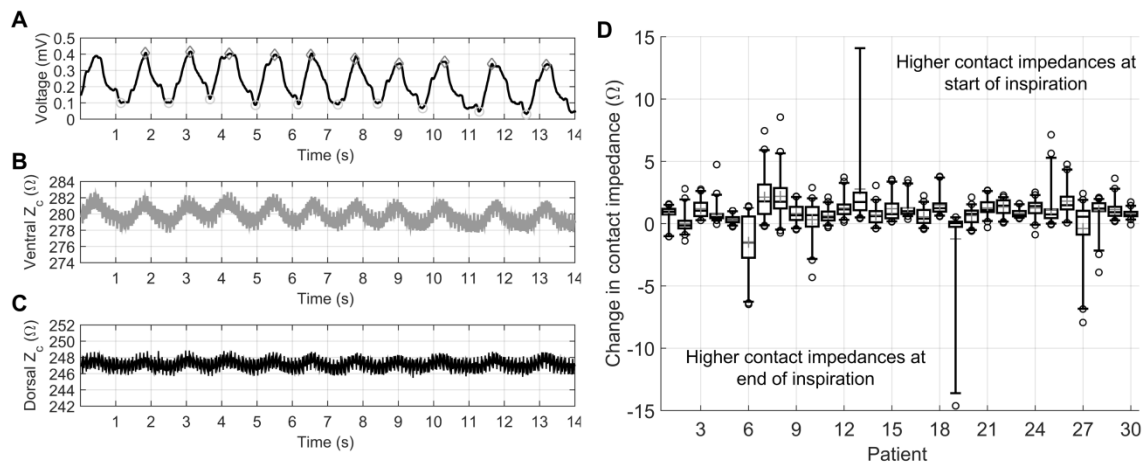


**Figure 4.** Example of contact impedance changes in a supine infant (body weight 1255 g, postnatal age 29.7 weeks, chest circumference 23.5 cm, belt size 20 cm, ventilation support: high-flow nasal cannula) in relation to the EIT ventilation signal (left) and the contact impedance changes at each electrode position of the whole study population (right). Panel A: The tidal ventilation signal of the patient, the starts and ends of inspiration are marked. Panels B and C: The ventral and dorsal contact impedances during tidal ventilation, respectively. Panel D: The contact impedance changes for each electrode and all 30 patients. Boxes indicate

25<sup>th</sup>-75<sup>th</sup> percentiles; the median is depicted by the line within the box, and the mean by a cross. The whiskers mark the 5<sup>th</sup> and 95<sup>th</sup> confidence interval.

The time course of contact impedance during 72 hours in one patient is presented in figure 5. The contact impedance of all electrodes was below 700 Ohm during most of the recording time. After 1 hour and 30 min the patient was turned to the left lateral position. The electrodes next to the sternum exhibited increased impedance thereafter. After turning the patient back to supine position at 5 hours of recording, all electrodes made good contact. During patient care the belt was readjusted and usually the contact impedance dropped after its completion. Between hour 27 and 29 the contact impedance of several electrodes was above 700 Ohm with a larger spread of the impedance values. A slight increase over time and then a drop of the impedance after each patient care intervention can be seen in the following sequence.

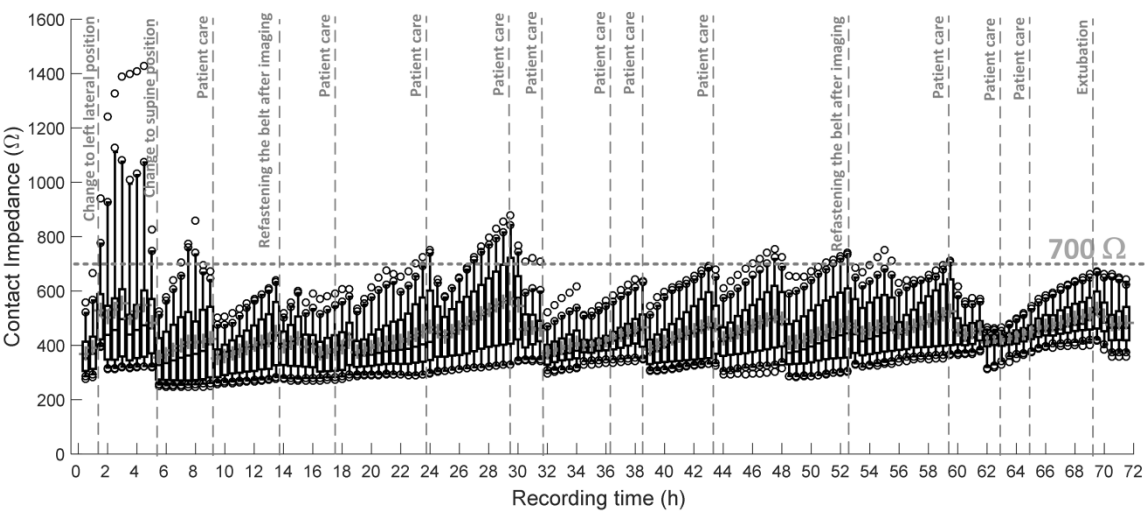


**Figure 5.** Contact impedance in one infant (body weight 2710 g, postnatal age 36.4 weeks, chest circumference 30 cm, belt size 27.5 cm) during 72 h of recording. Boxes indicate 25<sup>th</sup>-75<sup>th</sup> percentile; the median is depicted by the line within the box, and the mean by a cross. The whiskers mark the 5<sup>th</sup> and 95<sup>th</sup> confidence interval. Each boxplot summarises the contact impedance during 30 minutes of EIT recording. Changes in patient position, patient care, belt readjustment and extubation are marked in the time course. For the first 68 hours the infant was supported with high-frequency oscillatory ventilation, thereafter extubated and no ventilation support was provided.

During the 10 hours of recording the contact impedance increased from  $310 \pm 54$  Ohm (mean  $\pm$  SD) to  $420 \pm 62$  Ohm (figure 6). Thirty infants were measured during the first 3.5 hours; thereafter an increasing number of infants sequentially stopped EIT monitoring or needed re-application of gel. By 10 hours, data from only 9 infants was suitable for this analysis.



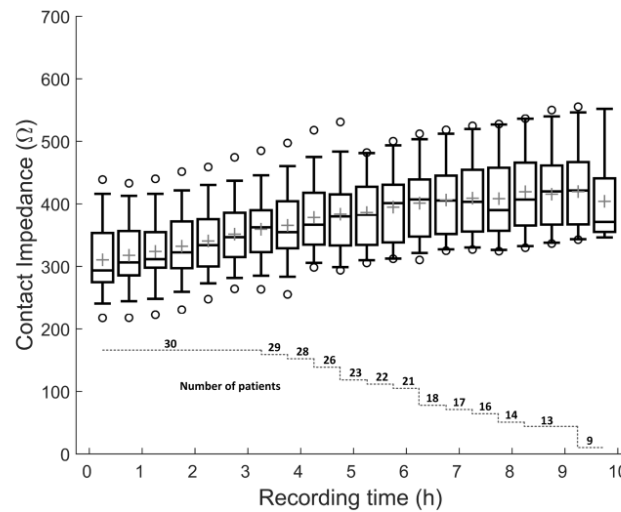


**Figure 6.** Increase in contact impedance during 10 hours of recording. The contact impedances for 30 minutes of recording for each patient are summarised in each boxplot. Boxes indicate 25<sup>th</sup>-75<sup>th</sup> percentiles, the median is depicted by the line within the box, and the means by a cross. The whiskers mark the 5<sup>th</sup> and 95<sup>th</sup> confidence interval. The number of patients is indicated below each boxplot in the bottom part of the diagram.

#### 4. Discussion

Until now, almost all neonatal EIT studies were performed with 16 single adhesive ECG electrodes (Frerichs *et al* 2003, Dunlop *et al* 2006, Riedel *et al* 2009, Schibler *et al* 2009, Miedema *et al* 2011, 2013). We developed a novel textile electrode interface for neonatal EIT measurement that enables a fast and accurate positioning of the electrodes around the chest. The proposed textile electrode belt has been used in two recent case reports (Miedema *et al* 2017, Oliva *et al* 2017) to measure regional ventilation distribution in a paediatric and a neonatal patient. In the present study we evaluated the clinical performance of the electrode belt in three university hospital NICUs in three European countries continuously over a period of up to three days.

Dry textile electrodes are not suitable for EIT measurements (Searle and Kirkup 2000, Puurtinen *et al* 2006, Waldmann *et al* 2017). While several fluids to reduce the contact impedance are available for adults, the selection of appropriate contact fluids for neonatal EIT application is more challenging. Healthy full-term infant's skin is well formed with a highly effective skin barrier, however the preterm skin has an underdeveloped skin barrier, with increased risk of skin damage, permeability and infections (Ågren *et al* 2006, Visscher and Narendran 2014). In this study the textile interface together with the gel caused minor redness of skin in only 6 out of 30 patients, which spontaneously resolved soon after belt removal. The skin irritation was not related to postnatal age or weight of the patient. In none of the patients the recording was interrupted or stopped because of the irritation. Our findings suggest that ultrasound gel together with the textile belt is well tolerated in infants and allows EIT monitoring up to three days.

The electrode interface described in Waldmann *et al* (2017) has an oblique shape and follows the sixth intercostal space of adult patients. However, comparing the ribcage of neonates and adults and its movement during breathing, the ribs of neonates are less inclined. Further, neonates show a stronger abdominal breathing pattern compared to adults (Ward *et al* 1992, Nagano *et al*

1997) Therefore, the used straight belt together with its adjustable soft closing mechanism allows the infants to breath naturally.

In our study, stable electrode-skin contact impedance was achieved immediately after fastening the electrode belt. Due to the fast application of the belt and the stable impedances, EIT monitoring could also be used in emergency situations such as resuscitation at birth (Tingay *et al* 2015, McCall *et al* 2017) where time and accuracy is crucial. This has not been possible with individual electrodes. In similar studies using ECG electrodes, several authors (Armstrong *et al* 2011, Miedema *et al* 2012, 2013, van der Burg *et al* 2014) described that electrodes had to be hand-trimmed before attaching them one by one to avoid short circuits between electrodes in small infants. This time consuming procedure is neither practical for daily clinical care nor very accurate.

The developed belt is not stretchable (only the closure stripe is), therefore the exact distance between each electrode is known. Together with the measured chest circumference, the exact electrode position can be calculated and used in the forward and inverse models (Boyle *et al* 2017). This is critical to image reconstruction accuracy, as wrong assumptions regarding the electrode position can lead to imaging errors (Lozano *et al* 1995, Tang *et al* 2002).

Since many of the EIT parameters, such as centre of ventilation (Frerichs *et al* 2006) global inhomogeneity index (Zhao *et al* 2009), anteroposterior ventilation ratio (Kunst *et al* 1999) and the so-called ‘silent spaces’ (Ukere *et al* 2016) are calculated by subtracting the impedance distribution at start of inspiration from the impedance distribution at end of inspiration, contact impedance changes during tidal ventilation need to be treated carefully. Uneven current injection amplitudes caused by the different contact impedances at the two described time points, could be misinterpreted as impedance changes within the body. Similarly to Boverman *et al* (2017) we reported a decrease in electrode contact impedance during inspiration and an increase during expiration in most of the electrodes. This change of contact impedance may be due to the slight stretching of the skin during in inspiration, which may expand pores through the epidermis (Boverman *et al* 2017).

Significantly higher contact impedances were measured in the ventral area compared with dorsal regions. Neonates were lying on the belt and therefore contact pressures were higher in the dorsal part. As described by Beckmann *et al* (2010) the contact impedance of textile interfaces is inversely proportional to the contact pressure – the higher the pressure the lower the contact impedances. Variations between the 32 contact impedances need to be taken into account and it is important that the current source of the EIT device provides constant current for different loads. Unequal current injection amplitude within one measurement cycle (32 current injections and 1024 voltage measurements) caused by different contact impedances, would influence the differential voltage measurements and therefore also the image reconstructions.

Boone and Holder (1996) concluded that fluctuations of contact impedance, between two measurement points, of less than 10 Ohm are required to reconstruct satisfactory images. We reported impedance changes less than 5 Ohm in most of the electrodes during tidal ventilation. Although contact impedance changes up to 15 Ohm were occasionally noted, compensation for these differences or eliminating measurements at these electrodes before reconstructing tidal images might be needed.

In 15 healthy men Takashima *et al* (2017) showed that the geometry of the thorax changes significantly in supine, lateral and sitting position. When changing the patient position from supine to lateral, the anteroposterior length increased and the mediolateral decreased. While single adhesive electrodes follow these shape changes, belt-like structures need not follow. As consequence, the deformation of the thorax may lead to high contact impedances and more failing electrodes. Due to the changes in geometry the belt should be refastened after repositioning of patients.

A slight increase in contact impedance was noticed over 10 hours. This is likely due to the used ultrasound gel which dries out over time (Ask *et al* 1979, Lozano *et al* 1995). Boone and Holder (1996) showed that a linear drift with a constant (i.e. all electrodes 100 Ohm) contact impedance did not cause any distortion of the reconstructed EIT images. Thus the contact impedance increase over time we observed and, described in figures 5 and 6 is unlikely to have a major influence on the EIT images.

Finally, we wish to address one minor limitation of the developed neonatal belt. It can be seen in the X-ray image, however, without causing any apparent major artefacts. The relatively large size of the belt in relation to small patient size may marginally hinder clinicians from identifying the underlying tissues.

## 5. Conclusion

We developed the first neonatal electrical impedance tomography electrode belt and tested its clinical long-term performance in a multicentre study. Low contact impedances and limited failing electrodes indicate that EIT measurements were possible most of the time. Further, our results show that the belt does not create any distress or discomfort for the neonatal patients. The ability to provide simple, fast and reproducible placement of the 32 electrodes opens new applications in the fields of neonatology.

## Acknowledgments

This project has received funding from the European Union's Horizon 2020 Research and Innovation Programme under the grant agreement No. 668259. Dr. Tingay is supported by a National Health and Medical Research Council Clinical Career Development Fellowship (Grant ID 11123859) and the Victorian Government Operational Infrastructure Support Program (Melbourne, Australia).

References

Adler, A., Amato, M.B., Arnold, J.H., Bayford, R., Bodenstein, M., Böhm, S.H., Brown, B.H., Frerichs, I., Stenqvist, O., Weiler, N., and Wolf, G.K., 2012. Whither lung EIT: Where are we, where do we want to go and what do we need to get there? *Physiological Measurement*, 33 (5), 679–694.

Adler, A., Grychtol, B., and Bayford, R., 2015. Why is EIT so hard, and what are we doing about it? *Physiological Measurement*, 36 (6), 1067–1073.

Ågren, J., Sjörs, G., and Sedin, G., 2006. Ambient humidity influences the rate of skin barrier maturation in extremely preterm infants. *Journal of Pediatrics*, 148 (5), 613–617.

Armstrong, R.K., Carlisle, H.R., Davis, P.G., Schibler, A., and Tingay, D.G., 2011. Distribution of tidal ventilation during volume-targeted ventilation is variable and influenced by age in the preterm lung. *Intensive Care Medicine*, 37 (5), 839–846.

Ask, P., Oberg, P.A., Odman, S., Tenland, T., and Skogh, M., 1979. ECG electrodes. A study of electrical and mechanical long-term properties. *Acta anaesthesiologica Scandinavica*, 23 (2), 189–206.

Bayford, R.H., 2006. Bioimpedance Tomography (Electrical Impedance Tomography). *Annual Review of Biomedical Engineering*, 8 (1), 63–91.

Beckmann, L., Neuhaus, C., Medrano, G., Jungbecker, N., Walter, M., Gries, T., and Leonhardt, S., 2010. Characterization of textile electrodes and conductors using standardized measurement setups. *Physiological measurement*, 31 (2), 233–47.

Boone, K.G. and Holder, D.S., 1996. Effect of skin impedance on image quality and variability in electrical impedance tomography: a model study. *Medical & biological engineering & computing*, 34 (5), 351–4.

Boverman, G., Isaacson, D., Newell, J.C., Saulnier, G.J., Kao, T.J., Amm, B.C., Wang, X., Davenport, D.M., Chong, D.H., Sahni, R., and Ashe, J.M., 2017. Efficient simultaneous reconstruction of time-varying images and electrode contact impedances in electrical impedance tomography. *IEEE Transactions on Biomedical Engineering*, 64 (4), 795–806.

Boyle, A. and Adler, A., 2011. The impact of electrode area, contact impedance and boundary shape on EIT images. *Physiological Measurement*, 32 (7), 745–754.

Boyle, A., Crabb, M.G., Jehl, M., Lionheart, W.R.B., and Adler, A., 2017. Methods for calculating the electrode position Jacobian for impedance imaging. *Physiological Measurement*, 38 (3), 555–574.

Brown, B.H., Barber, D.C., and Seagar, A.D., 1985. Clinical Physics and Physiological Measurement Applied potential tomography: possible clinical adpplications. *Clin. Phys. Physiol. Meas. Physiol. Meas*, 6 (2), 109–121.

van der Burg, P.S., Miedema, M., de Jongh, F.H., Frerichs, I., and van Kaam, A.H., 2014. Cross-sectional changes in lung volume measured by electrical impedance tomography are representative for the whole lung in ventilated preterm infants. *Critical care medicine*, 42 (6), 1524–30.

Chatziioannidis, I., Samaras, T., and Nikolaidis, N., 2011. Electrical impedance tomography: A new study method for neonatal respiratory distress syndrome? *Hippokratia*, 15 (3), 211–215.

Dunlop, S., Hough, J., Riedel, T., Fraser, J.F., Dunster, K., and Schibler, A., 2006.

Electrical impedance tomography in extremely prematurely born infants and during high frequency oscillatory ventilation analyzed in the frequency domain.

*Physiological measurement*, 27 (11), 1151–1165.

- Frerichs, I., Amato, M.B.P., van Kaam, A.H., Tingay, D.G., Zhao, Z., Grychtol, B., Bodenstein, M., Gagnon, H., Böhm, S.H., Teschner, E., Stenqvist, O., Mauri, T., Torsani, V., Camporota, L., Schibler, A., Wolf, G.K., Gommers, D., Leonhardt, S., Adler, A., and TREND study group, 2017. Chest electrical impedance tomography examination, data analysis, terminology, clinical use and recommendations: consensus statement of the TRanslational EIT developmeNt stuDy group. *Thorax*, 72 (1), 83–93.
- Frerichs, I., Dargaville, P.A., Van Genderingen, H., Morel, D.R., and Rimensberger, P.C., 2006. Lung volume recruitment after surfactant administration modifies spatial distribution of ventilation. *American Journal of Respiratory and Critical Care Medicine*, 174 (7), 772–779.
- Frerichs, I., Schiffmann, H., Oehler, R., Dudykevych, T., Hahn, G., Hinz, J., and Hellige, G., 2003. Distribution of lung ventilation in spontaneously breathing neonates lying in different body positions. *Intensive Care Med*, 29, 787–794.
- Hampshire, a R., Smallwood, R.H., Brown, B.H., and Primhak, R. a, 1995. Multifrequency and parametric EIT images of neonatal lungs. *Physiological measurement*, 16 (3A), A175-89.
- Kunst, P.W.A., De Vries, P.M.J.M., Postmus, P.E., and Bakker, J., 1999. Evaluation of electrical impedance tomography in the measurement of PEEP-induced changes in lung volume. *Chest*, 115 (4), 1102–1106.
- Lozano, A., Rosell, J., and Pallás-Areny, R., 1995. Errors in prolonged electrical impedance measurements due to electrode repositioning and postural changes. *Physiological measurement*, 16, 121–130.
- McAdams, E.T., Jossinet, J., Lacknermeier, A., and Risacher, F., 1996. Factors affecting electrode-gel-skin interface impedance in electrical impedance tomography. *Medical & biological engineering & computing*, 34 (6), 397–408.
- McCall, K.E., Waldmann, A.D., Pereira-Fantini, P., Oakley, R., Miedema, M., Perkins, E.J., Davis, P.G., Dargaville, P.A., Böhm, S.H., Dellacà, R., Sourial, M., Zannin, E., Rajapaksa, A.E., Tan, A., Adler, A., Frerichs, I., and Tingay, D.G., 2017. Time to lung aeration during a sustained inflation at birth is influenced by gestation in lambs. *Pediatric Research*, 82 (4), 712–720.
- Miedema, M., van der Burg, P.S., Beuger, S., de Jongh, F.H., Frerichs, I., and van Kaam, A.H., 2013. Effect of nasal continuous and biphasic positive airway pressure on lung volume in preterm infants. *The Journal of pediatrics*, 162 (4), 691–7.
- Miedema, M., de Jongh, F.H., Frerichs, I., van Veenendaal, M.B., and van Kaam, A.H., 2011. Changes in lung volume and ventilation during surfactant treatment in ventilated preterm infants. *American journal of respiratory and critical care medicine*, 184 (1), 100–5.
- Miedema, M., de Jongh, F.H., Frerichs, I., van Veenendaal, M.B., and van Kaam, A.H., 2012. Regional respiratory time constants during lung recruitment in high-frequency oscillatory ventilated preterm infants. *Intensive care medicine*, 38 (2), 294–9.
- Miedema, M., Waldmann, A., McCall, K.E., Böhm, S.H., van Kaam, A.H., and Tingay, D.G., 2017. Individualized Multiplanar Electrical Impedance Tomography in Infants

- to Optimize Lung Monitoring. *American Journal of Respiratory and Critical Care Medicine*, 195 (4), 536–538.
- Nagano, O., Ohta, Y., and Hirakawa, M., 1997. Pressure Support Ventilation Augments Spontaneous Breathing with Improved Thoracoabdominal Synchrony Neonates with Congenital Heart Disease.
- Oliva, P. de la, Waldmann, A.D., Böhm, S.H., Verdú-Sánchez, C., Pérez-Ferrer, A., and Alvarez-Rojas, E., 2017. Bedside Breath-Wise Visualization of Bronchospasm by Electrical Impedance Tomography Could Improve Perioperative Patient Safety: A Case Report. *A & A Case Reports*, 8, 1–4.
- Puurtinen, M.M., Komulainen, S.M., Kauppinen, P.K., Malmivuo, J.A. V., and Hyttinen, J.A.K., 2006. Measurement of noise and impedance of dry and wet textile electrodes, and textile electrodes with hydrogel. In: *2006 International Conference of the IEEE Engineering in Medicine and Biology Society*. IEEE, 6012–6015.
- Rahal, M., Khor, J.M., Demosthenous, A., Tizzard, A., and Bayford, R., 2009. A comparison study of electrodes for neonate electrical impedance tomography. *Physiological Measurement*, 30 (6), S73–S84.
- Riedel, T., Kyburz, M., Latzin, P., Thamrin, C., and Frey, U., 2009. Regional and overall ventilation inhomogeneities in preterm and term-born infants. *Intensive Care Medicine*, 35 (1), 144–151.
- Schibler, A., Yuill, M., Parsley, C., Pham, T., Gilshenan, K., and Dakin, C., 2009. Regional ventilation distribution in non-sedated spontaneously breathing newborns and adults is not different. *Pediatric Pulmonology*, 44 (9), 851–858.
- Searle, A. and Kirkup, L., 2000. A direct comparison of wet, dry and insulating bioelectric recording electrodes. *Physiological Measurement*, 21 (2), 271–283.
- Takashima, S., Nozoe, M., and Mase, K., 2017. Effects of posture on chest-wall configuration and motion during tidal breathing in normal men, 29–34.
- Taktak, A., Record, P., Gadd, R., and Rolfe, P., 1995. Practical factors in neonatal lung imaging using electrical impedance tomography. *Medical & Biological Engineering & Computing*, 33 (2), 202–205.
- Tang, M., Wang, W., Wheeler, J., McCormick, M., and Dong, X., 2002. Effects of incompatible boundary information in EIT on the convergence behavior of an iterative algorithm. *IEEE Transactions on Medical Imaging*, 21 (6), 620–628.
- Tingay, D.G., Lavizzari, A., Zonneveld, C.E.E., Rajapaksa, A.E., Zannin, E., Perkins, E., Black, D., Sourial, M., Dellacà, R.L., Mosca, F., Adler, A., Grychtol, B., Frerichs, I., and Davis, P.G., 2015. An Individualized Approach To Sustained Inflation Duration At Birth Improves Outcomes In Newborn Preterm Lambs. *American Journal of Physiology - Lung Cellular and Molecular Physiology*, ajplung.00277.2015.
- Ukere, A., März, A., Wodack, K.H., Trepte, C.J., Haese, A., Waldmann, A.D., Böhm, S.H., and Reuter, D.A., 2016. Perioperative assessment of regional ventilation during changing body positions and ventilation conditions by electrical impedance tomography. *British Journal of Anaesthesia*, 117 (2), 228–235.
- Visscher, M. and Narendran, V., 2014. Neonatal Infant Skin: Development, Structure and Function, 14, 135–141.
- Waldmann, A.D., Wodack, K.H., März, A., Ukere, A., Trepte, C.J., Böhm, S.H., and Reuter, D.A., 2017. Performance of Novel Patient Interface for Electrical Impedance Tomography Applications. *Journal of Medical and Biological Engineering*, 37 (4),

561–566.

Ward, M.E., Ward, J.W., and Macklem, P.T., 1992. Analysis of human chest wall motion using a two-compartment rib cage model. *Journal of applied physiology (Bethesda, Md. : 1985)*, 72 (4), 1338–47.

Zhao, Z., Müller, K., Steinmann, D., Frerichs, I., and Guttman, J., 2009. Evaluation of an electrical impedance tomography-based global inhomogeneity index for pulmonary ventilation distribution. *Intensive Care Medicine*, 35 (11), 1900–1906.

Appendix

Questionnaire: “Evaluation of the EIT belt during the CRADL project“.

User information

Profession	Institution	Date
<input type="checkbox"/> nurse <input type="checkbox"/> physician <input type="checkbox"/> other: _____		

Patient information

Age	Weight	Gender	Thorax circumference

Material used

Belt size
Contact Agent
<input type="checkbox"/> Ultrasound gel <input type="checkbox"/> Swisstom Contact Agent <input type="checkbox"/> Other: _____

Questions:

- 1) How many clinicians were involved in:  
- applying the Contact Agent?  
\_\_\_\_\_  
  
- fastening the belt on the patient?  
\_\_\_\_\_
- 2) For how long did you acquire EIT data on this patient?  
\_\_\_\_\_
- 3) Did you adjust the Sensor Belt position (without fully removing it) or reattach the velcro because you felt that the belt restricted the breathing of the patient?  
☐ agree  
☐ rather agree  
☐ neither agree nor disagree  
☐ rather disagree  
☐ disagree

Comments:

\_\_\_\_\_



4) Did you temporarily remove the Sensor Belt during the examination

☐ yes ☐ no

If yes for which reason (multiple answers are allowed):

- ☐ nursing
- ☐ Kangaroo care
- ☐ skin condition
- ☐ improvement of Sensor Belt position
- ☐ reapplication of Contact Agent
- ☐ suspected breathing restriction
- ☐ Other

Comments:

---

5) Did you observe any skin irritations when removing the Sensor Belt? If yes, which ones?

☐ no ☐ minor, please describe ☐ severe, please describe

---

6) Did you stop the examination because you felt that the Sensor Belt restricted the ventilation?

☐ yes ☐ no

7) Comments and suggestions:

---